

# Evaluation of Figures of Merit for Colorimetric Cameras

Michael Vrhel

Artifex Software, Novato, CA 94945, USA

E-mail: michael.vrhel@artifex.com

H. Joel Trussell

North Carolina State University, Department of Electrical and Computer Engineering, Raleigh, NC 27606, USA

**Abstract.** We investigate the relationship between goodness measures of spectral sensitivities to actual  $\Delta E$  performance in the presence of signal dependent noise. We show that the Vora value does not perform as well as Sharma's figure of merit (FOM). In addition, we show that Sharma's FOM has issues when the spectral samples include lower luminance data. We introduce an FOM that accounts for signal dependent noise and has a linear relationship to  $\Delta E$  performance. The improvement introduced by including signal dependent noise in the FOM results in closer relationships of the FOM to colorimetric accuracy in all cases but is especially important when the ensemble under investigation has a wide range of luminance values. © 2022 Society for Imaging Science and Technology.  
[DOI: 10.2352/J.ImagingSci.Technol.2022.66.5.050402]

## 1. INTRODUCTION

Creating a robust design of the spectral sensitivity of a color measuring device such as a camera, scanner, or colorimeter requires several considerations. These include accounting for existing optical elements in the design such as lenses, IR filters, and sensor quantum efficiency; realizability of color filters; recording illumination; variability of spectral characteristics in manufacturing; and system noise. In the design and evaluation of these devices, it is efficient to use a figure of merit (FOM) or goodness measure that is closely correlated with perceived color accuracy [1–9]. The FOMs are usually developed to obtain high correlation with various  $\Delta E$  averages in the CIELAB color space. The advantage of using an FOM is that its computation is considerably less than simulating the average  $\Delta E$  over an ensemble of spectra under realistic noise conditions. Of course, as we show, the development of effective FOMs requires such simulations. Once the FOM is developed, it is easy to use it to compare different devices or even optimize them.

Typically in formulating a camera design problem, a mathematical model is used for the device imaging process such as the following

$$\mathbf{c} = \mathbf{H}^T \mathbf{O} \mathbf{r} + \mathbf{n}, \quad (1)$$

where the visible spectrum has been mathematically sampled at  $N$  wavelengths [10]. The  $N \times M$  dimension matrix  $\mathbf{H}$

contains the  $M$  spectral sensitivities of the device that we wish to design; the diagonal matrix  $\mathbf{O}$  contains the concatenated spectral sensitivities of the other elements of the device (e.g., lens, IR filter, sensor efficiency); the  $N$ -element vector  $\mathbf{r}$  represents the radiant spectrum that is measured by the device; the  $M$ -element vector  $\mathbf{n}$  is zero mean, additive noise; and the  $M$ -element vector  $\mathbf{c}$  is the value measured by the device. To simplify things, we will combine the matrix  $\mathbf{H}$  and the matrix  $\mathbf{O}$  into an  $N \times M$  matrix  $\mathbf{G}$ , giving us

$$\mathbf{c} = \mathbf{G}^T \mathbf{r} + \mathbf{n}. \quad (2)$$

Note that the radiant spectrum  $\mathbf{r}$  entering the camera can be broken down into an illuminant and a reflectance component. The illuminant is of importance when considering the mapping to CIE values.

To facilitate the design process, we wish to quantify the goodness of the overall system spectral sensitivity given by the matrix  $\mathbf{G}$ . Such a goodness measure, can be used to determine a matrix  $\mathbf{H}$  that provides the “best” color measuring results. Depending upon the approach, the matrix  $\mathbf{H}$  is analytically determined with constraints on realizability (e.g., nonnegativity, smoothness) [11–15], parametric models (e.g. Gaussian shapes) [2, 4, 16, 17], or selected from a set of readily available filters [8, 18, 19]. Regardless of the approach used, the use of a measure to quantify how well a filter set performs relative to the goodness measure is of use.

Here we compare how well different FOMs correlate to  $\Delta E$  performance for a number of cameras. For each camera, simulated raw camera values of spectral samples are transformed to CIEXYZ values using the linear minimum mean square error estimator. The camera model includes signal dependent noise. In computing the  $\Delta E$  value on each spectral sample, we average over a large number of signal dependent noise realizations. The resulting  $\Delta E$  values from the spectral samples are averaged. The correlations are then computed between averaged  $\Delta E$  and FOMs for the collection of cameras.

## 2. FIGURES OF MERIT

There are several measures that have been proposed to quantify the goodness of the spectral sensitivity of a color measuring device. These measures were developed to

measure how well the device performs in providing accurate CIE color measurements obtained by the linear minimum mean square error (LMMSE) method. Using notation similar to above, the CIEXYZ vector for the radiant spectrum  $\mathbf{r}$  can be expressed as

$$\mathbf{t}(\mathbf{r}) = \mathbf{A}^T \mathbf{r}, \quad (3)$$

where the  $N \times 3$  matrix  $\mathbf{A}$  contains the sample CIEXYZ color matching functions, and the three element vector  $\mathbf{t}(\mathbf{r})$  is the CIEXYZ value of the radiant spectrum  $\mathbf{r}$ . Again this radiant spectrum can be decomposed into an illuminant and reflection component, and the illuminant will define the white point to which we would map to CIELAB. In this work, we assume a spectrally uniform illuminant. There are measures that consider multiple illuminants [3] as well as work that considers the problem of capturing data for multiple illuminants [12]. Here we are focused on comparing measures of goodness for a single illuminant.

The earliest measure for quantifying the goodness of a single color filter  $\mathbf{m}$  is Neugebauer's q-factor [20]. Mathematically, this measure is given by

$$q(\mathbf{m}) = \frac{\|P_A \mathbf{m}\|^2}{\|\mathbf{m}\|^2}, \quad (4)$$

where  $P_A$  is the orthogonal projection operator onto the subspace defined by the matrix  $\mathbf{A}$ . The projection operator can be determined from

$$P_A = \mathbf{A}(\mathbf{A}^T \mathbf{A})^{-1} \mathbf{A}^T. \quad (5)$$

The q-factor is bounded between 0.0 and 1.0, with a value of 0.0 indicating that the filter  $\mathbf{m}$  lies totally outside (is orthogonal to) the subspace defined by the CIE color matching functions and 1.0 indicating that the filter lies completely inside the subspace. Note that the q-factor only provides the measure of a single filter. This single filter constraint is a shortcoming of the q-factor, as we require a measure that quantifies the entire system response that is defined by the matrix  $\mathbf{G}$  in Eq. (2). For example, we could select three filters that are each contained in the subspace defined by matrix  $\mathbf{A}$  giving optimal q-factor values of 1.0 for each filter. However, when the filters are combined, it is possible that they do not span the full three-dimensional subspace defined by the matrix  $\mathbf{A}$ .

The Vora value [21] solves this issue and is given by

$$v(\mathbf{A}, \mathbf{G}) = \frac{\text{Trace}[P_A P_G]}{3}, \quad (6)$$

where  $P_G$  is the orthogonal projection operator onto the subspace defined by the system response that we wish to quantify, and can be computed in the same manner as Eq. (5). Similar to the q-factor, the Vora value ranges from 0.0 to 1.0 with 0.0 indicating that the subspaces defined by the matrix  $\mathbf{A}$  and  $\mathbf{G}$  do not overlap (are orthogonal) and 1.0 indicating that the subspaces are the same. The Vora value does not consider the spectral data that is being measured, nor does it account for system noise. Sharma proposed several FOMs

that account for these parameters [5]. Sharma assumes the use of a LMMSE estimator in his FOMs.

The most complex FOM proposed by Sharma is given by

$$q_{\mathcal{F}}(\mathbf{A}, \mathbf{G}) = \frac{\tau(\mathbf{A}, \mathbf{G})}{\alpha(\mathbf{A})}, \quad (7)$$

where the denominator is given by

$$\alpha(\mathbf{A}) = \text{vec}(\mathbf{A}^T)^T \mathbf{S}_r \text{vec}(\mathbf{A}^T), \quad (8)$$

and  $\mathbf{S}_r$  is mathematically defined below and is an autocorrelation matrix related to the reflectance or radiant spectra, but in the perspective CIELAB color space.

The numerator is given by

$$\begin{aligned} \tau(\mathbf{A}, \mathbf{G}) &= \text{vec}(\mathbf{A}^T)^T \mathbf{S}_r (\mathbf{G} \otimes \mathbf{I}_3) \\ &\quad \times [(\mathbf{G}^T \otimes \mathbf{I}_3) \mathbf{S}_r (\mathbf{G} \otimes \mathbf{I}_3) + \mathbf{S}_n]^{-1} \\ &\quad \times (\mathbf{G}^T \otimes \mathbf{I}_3) \mathbf{S}_r \text{vec}(\mathbf{A}^T), \end{aligned} \quad (9)$$

where  $\mathbf{S}_n$  is mathematically defined below and is a weighted version of the noise autocorrelation matrix. The symbol  $\otimes$  represents the Kronecker product.

To complete the definition of the FOM, the autocorrelation matrix terms are given by

$$\mathbf{S}_r = E\{(\mathbf{r}\mathbf{r}^T) \otimes (J_{\mathcal{F}}^T(\mathbf{t}(\mathbf{r}))J_{\mathcal{F}}(\mathbf{t}(\mathbf{r})))\}, \quad (10)$$

$$\mathbf{S}_n = \mathbf{K}_n \otimes E\{J_{\mathcal{F}}^T(\mathbf{t}(\mathbf{r}))J_{\mathcal{F}}(\mathbf{t}(\mathbf{r}))\}, \quad (11)$$

$$\mathbf{K}_n = E\{\mathbf{m}\mathbf{m}^T\}, \quad (12)$$

where  $J_{\mathcal{F}}(\mathbf{t}(\mathbf{r}))$  is the Jacobian matrix of the transformation to CIELAB space for the CIEXYZ value  $\mathbf{t}(\mathbf{r})$ .

Note that the above FOM requires the statistical characterization of the ensemble of spectra  $\{\mathbf{r}\}$ , assumes signal independent noise, and also assumes that a minimum linear least squares estimator is used for mapping the measured value to CIEXYZ values. In this FOM, through the use of the Jacobian matrix, a first order Taylor approximation is made at each reflectance value to account for the transformation to CIELAB from CIEXYZ, which provides a perceptually more meaningful measure. Such an approximation was introduced by Wolski for the design of color filters [14]. See Appendix C of Sharma [5] or Eq. (4) of Wolski [14] for details on computing the Jacobian.

In practice, the noise model for a color measuring instrument is not signal independent but is signal dependent. While the noise is signal dependent, it is uncorrelated with the signal. The recorded measurement value can be well modeled with a Poisson distribution [8, 16, 22]. A characteristic of a Poisson distribution is that its mean is equal to its variance. In our case, due to the large number of photons that arrive at the sensor, we can model the mean value as the noise-free measurement, and the noise as a Gaussian distribution that has a zero mean with a variance that is a scaled factor of the measured value. The scaling occurs due to the existence of gain in the system. A system gain of  $\gamma$  on a measured component will scale the noise-free value by  $\gamma$  but scale the variance by  $\gamma^2$ ,

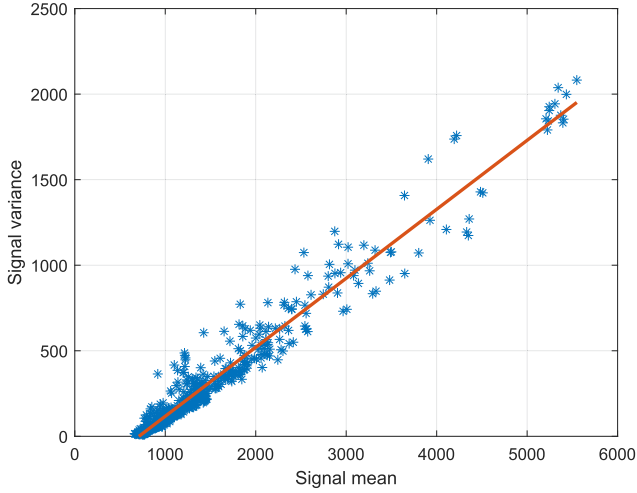


Figure 1. Signal mean versus signal variance for Nikon D750. Slope of fitted line is  $\gamma = 0.4$ .

introducing a scale factor of  $\gamma$  between the Poisson mean and variance. It is straight-forward to determine the scale factor for a particular device through the measurement of known reflectance samples [22]. Figure 1 provides an example case, where a Nikon D750 camera was used to measure samples of spatially constant reflectance. Here we plot the mean value of the sample versus the variance within the sample. The slope of the linear fit to the data (shown as a red line) indicates the scaling factor ( $\gamma$  value) that should be used for the noise model for a channel of the camera, which is approximately  $\gamma = 0.4$  as shown by the fitted line in the figure. It is common to see scale factors of  $\gamma = 0.4$  to 0.8 in cameras that we have investigated.

It is possible to adjust the FOM given in Eq. (7) to account for a signal dependent noise model. The adjustment involves performing a modification of Eq. (11). Instead, we use

$$\mathbf{S}_{sd} = E\{\mathbf{n}(\mathbf{r})\mathbf{n}(\mathbf{r})^T\} \otimes J_{\mathcal{F}}^T(\mathbf{t}(\mathbf{r}))J_{\mathcal{F}}(\mathbf{t}(\mathbf{r})), \quad (13)$$

where  $\mathbf{n}(\mathbf{r})$  represents the realization of a signal dependent noise value when measuring the radiant spectrum  $\mathbf{r}$ . Note that the variance of the noise is dependent upon the value of  $\mathbf{r}$ . The value  $\mathbf{S}_{sd}$  is used in place of  $\mathbf{S}_n$  in the computation of the value for  $\tau$  given in Eq. (9).

In practice, the values of  $\mathbf{S}_{sd}$ ,  $\mathbf{S}_r$ , and  $\mathbf{S}_n$  are estimated from an ensemble of selected spectra. Assuming that we have a collection of  $P$  spectra, estimates for each of these terms are given by

$$\tilde{\mathbf{S}}_r = \frac{1}{P} \sum_{i=1}^P (\mathbf{r}_i \mathbf{r}_i^T) \otimes (J_{\mathcal{F}}^T(\mathbf{t}(\mathbf{r}_i))J_{\mathcal{F}}(\mathbf{t}(\mathbf{r}_i))), \quad (14)$$

$$\tilde{\mathbf{S}}_n = \frac{1}{P} \mathbf{K}_n \otimes \sum_{i=1}^P J_{\mathcal{F}}^T(\mathbf{t}(\mathbf{r}_i))J_{\mathcal{F}}(\mathbf{t}(\mathbf{r}_i)), \quad (15)$$

and

$$\tilde{\mathbf{S}}_{sd} = \frac{1}{P} \sum_{i=1}^P (\mathbf{K}_n(\mathbf{r}_i)) \otimes J_{\mathcal{F}}^T(\mathbf{t}(\mathbf{r}_i))J_{\mathcal{F}}(\mathbf{t}(\mathbf{r}_i)), \quad (16)$$

where  $\mathbf{K}_n(\mathbf{r}_i)$  is the autocorrelation matrix of the noise when measuring the radiance spectrum  $\mathbf{r}_i$ . When computing the value of  $\tilde{\mathbf{S}}_{sd}$ , the autocorrelation matrix  $\mathbf{K}_n(\mathbf{r}_i)$  is known from the camera model. For example, if the  $M$  channel noise slopes due to the system gain are given by  $\boldsymbol{\gamma} = [\gamma_1, \dots, \gamma_M]^T$  and

$$\mathbf{d}_i = \mathbf{G}^T \mathbf{r}_i \quad (17)$$

is the noise-free measurement, then

$$\mathbf{K}_n(\mathbf{r}_i) = \text{diag}(\mathbf{d}_i \odot \boldsymbol{\gamma}), \quad (18)$$

where  $\odot$  represents the Hadamard product, and  $\text{diag}(\cdot)$  is an operator that creates a diagonal matrix from a vector.

In addition to accounting for signal dependent noise, it is useful if an FOM is linearly related to the  $\Delta E$  performance of the device. Sharma noted that the FOM he developed has a  $\sqrt{1 - \text{FOM}}$  relationship to  $\Delta E$ , which is clearly nonlinear [5]. To achieve a measure that linearly relates to  $\Delta E$  performance, we can apply a correction factor to the FOM measure that is given by

$$1 - \sqrt{1 - \text{FOM}}. \quad (19)$$

This correction ensures that the measure remains between 0.0 and 1.0 with a value of 0.0 indicating a poor measure and a measure of 1.0 indicating a perfect measure. This same adjustment was suggested by Quan et al. where they altered Sharma's FOM measures to account for cross illumination mappings [3].

### 3. COMPARISON OF MEASURES

Given the above measures, our focus is to compare their ability to quantify the color accuracy of a camera. To investigate this, we used two data bases of camera spectral sensitivities, and four spectral reflectance/radiance data sets. The sensitivity data bases consisted of a database from RIT [23] that contained 28 cameras and a database of 20 phone cameras [24]. The spectral databases include reflectivities of a textile database [25] (4827 samples), an X-Rite SG chart (140 samples), a Digieye DT chart (240 samples), and a set of radiant spectra measured *in situ* (2262 samples) [26]. We computed  $\Delta E$  values that resulted from the LMMSE method for each data set with each camera for a level of signal dependent noise that was given by a scale factor of 0.8 in each of the color channels. In this computation, we used the LMMSE estimator that was based upon the known components of the device model. The signal dependent noise model was handled in the same manner as was used in Trussell and Shamey [27]. It was not necessary to perform a regression data fit, since the model components are known exactly. Note that we used  $\Delta E$  and not  $\Delta E_{2000}$  as the error metric. The reason is that the Jacobian matrix  $J_{\mathcal{F}}(\mathbf{t}(\mathbf{r}))$  used in Sharma's original measure does not account for the weighting that is used in the computation of the  $\Delta E_{2000}$  error metric. At this point, we want to use Sharma's original calculation, which assumes a uniform error weighting in the CIELAB components.

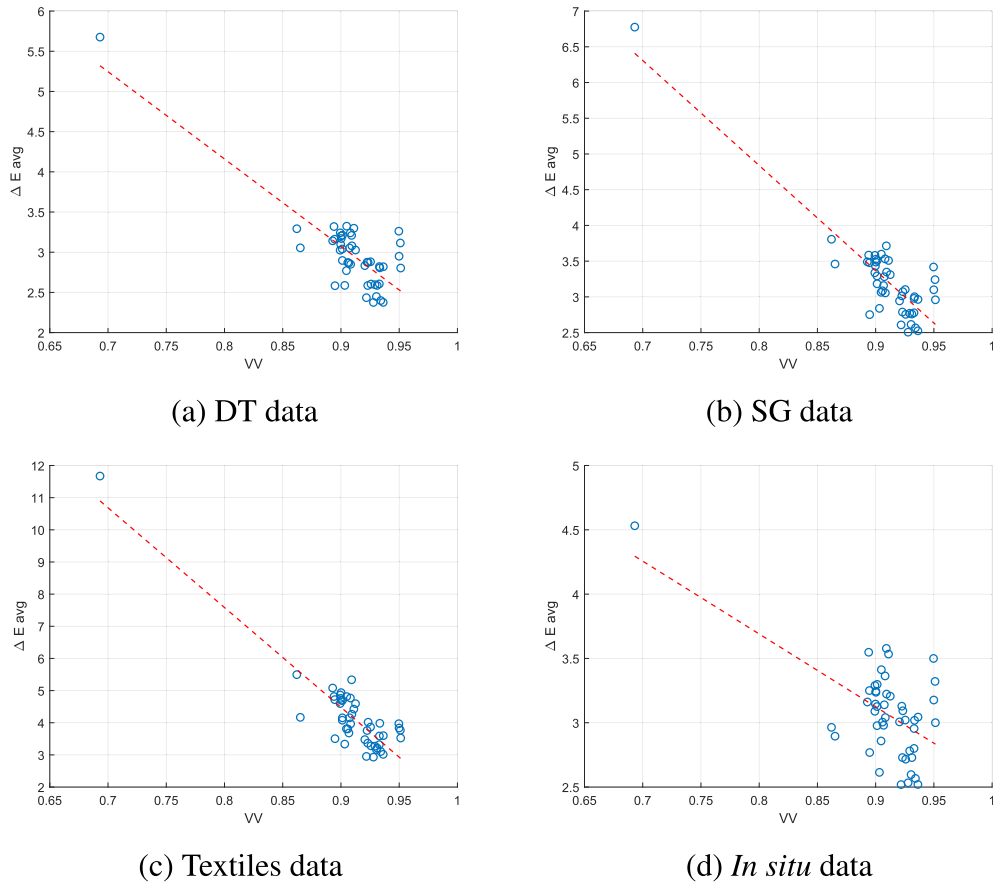


Figure 2. Vora value versus  $\Delta E$  at a noise slope of  $\gamma = 0.8$ .

These average  $\Delta E$  values for each camera are compared to the previously discussed FOMs. To do this, we computed the Vora value for each camera. In addition, we computed the FOM value given by Eq. (7) for each camera and data set combination assuming signal independent noise given at a level that was the average of the signal dependent noise across the data set. Finally, we computed the new FOM measure that accounted for signal dependent noise (using Eq. (16)) and included the nonlinear adjustment. For completeness, and to enable the ability to determine the usefulness of accounting for signal dependent noise, we also computed the original FOM value given by Eq. (7) but with the nonlinear adjustment applied to it, to provide a linear relationship to  $\Delta E$ . To compute the  $\Delta E$  performance of each camera, it is necessary to run a large number of noise simulations. We used 1000 noise realizations for every spectral sample across all the cameras.

We present the results in several different plots. Figure 2 shows how the Vora values of the cameras relate to the simulated  $\Delta E$  performance for each of the spectral data sets. The dashed line is the least squares linear fit to the data. From these plots, we see that the Vora value struggles in providing a clear relationship to  $\Delta E$ . While there is one outlier camera that clearly has poor performance in terms of  $\Delta E$  and the Vora value, the remaining cameras show limited correlation between  $\Delta E$  and the Vora value. Many cameras result in the

same Vora value but have significantly different average  $\Delta E$  performance numbers. While useful for cases where there is no spectral information about the data being measured, it may not be as useful for cases that employ such information. For our remaining comparisons, we will remove the outlier camera, since all the FOMs also identified the camera as producing very poor colorimetric accuracy.

Figure 3 shows the results of using Sharma's FOM as it was originally defined for the four spectral data sets. The FOM and  $\Delta E$  axes have the same scaling to indicate dependency of the FOM on the data sets. Figure 4 show the same results but with the nonlinear adjustment applied to the FOM values. As before, we show the least squares linear fit to the data. In addition, the correlation coefficient for each fit is provided. The FOM values show an improvement compared to the Vora values in terms of having a correlation with  $\Delta E$ . Comparison of the correlation coefficients between Figs. 3 and 4 show only a slight improvement obtained by the application of the nonlinear adjustment. Comparison of the four data sets show that the *in situ* data set [26] FOM results (both adjusted and non-adjusted) are quite different in nature from the other three data sets. In addition, the correlation coefficient is lower for the *in situ* data set, implying the discrimination of cameras with different  $\Delta E$  performance numbers is not very good in Fig. 4(d).

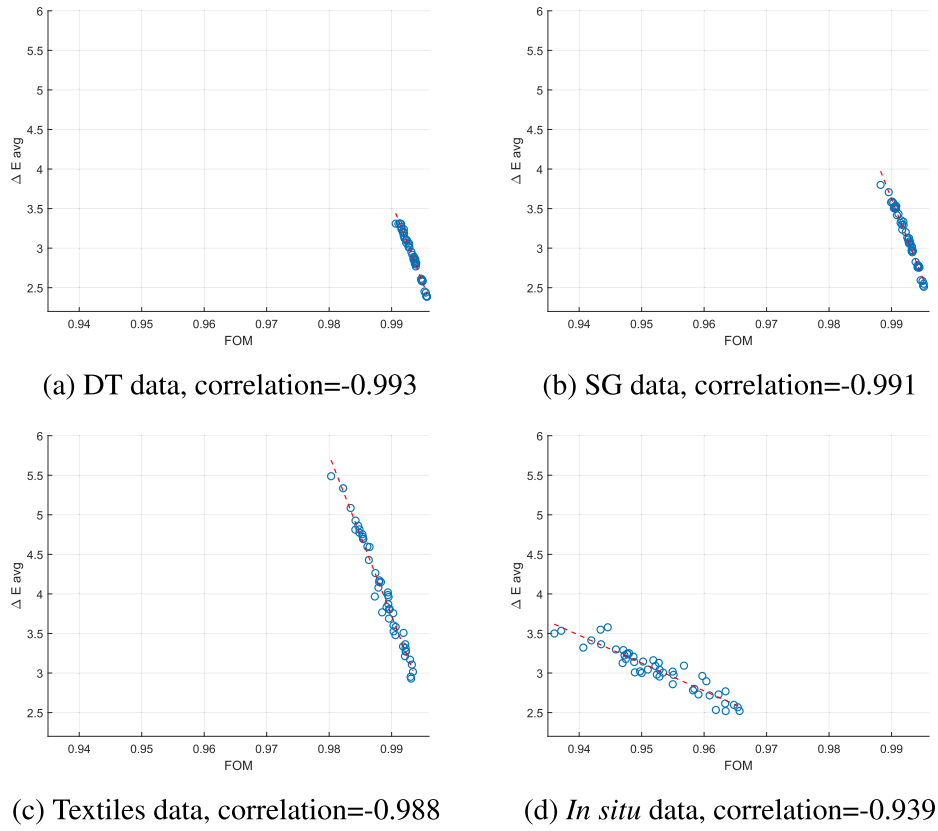


Figure 3. Sharma's FOM versus  $\Delta E$  at a noise slope of  $\gamma = 0.8$ .

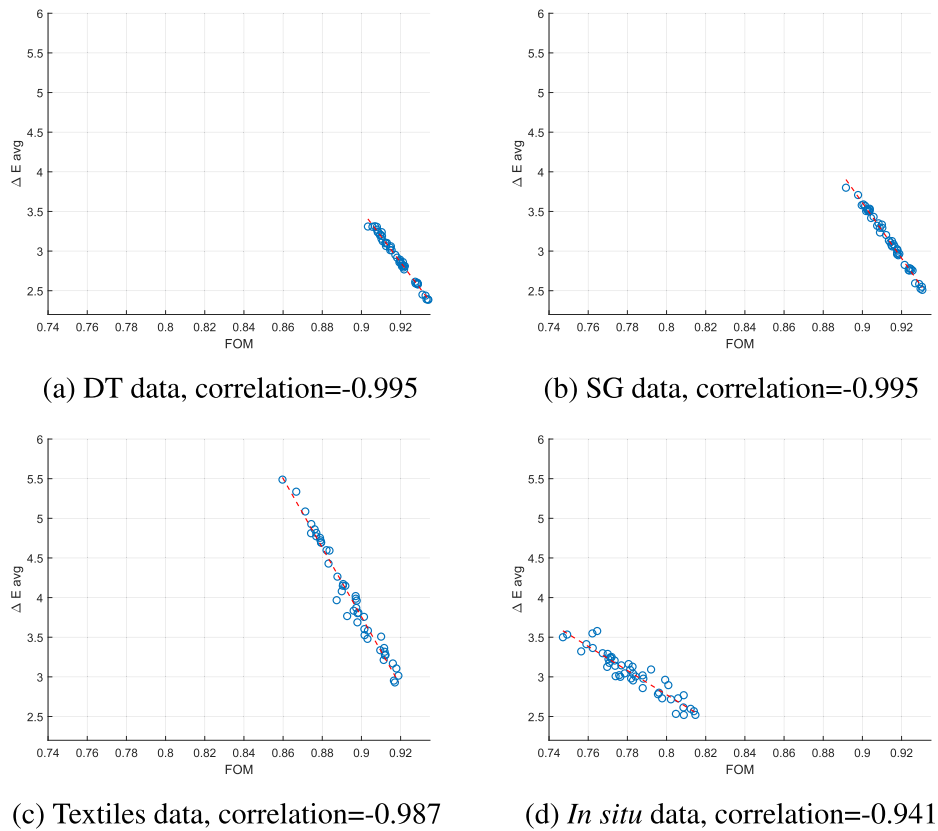
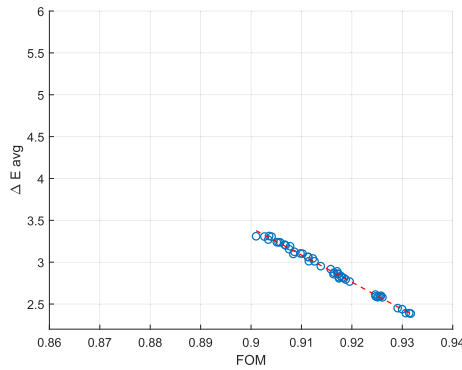
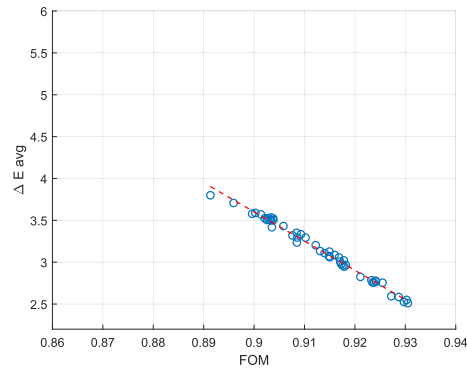


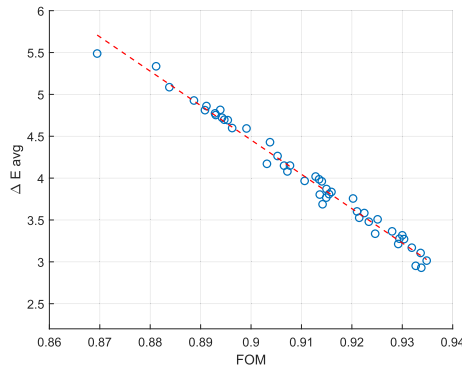
Figure 4. Sharma's FOM with nonlinear adjustment versus  $\Delta E$  at a noise slope of  $\gamma = 0.8$ .



(a) DT data, correlation=-0.997



(b) SG data, correlation=-0.995



(c) Textiles data, correlation=-0.992

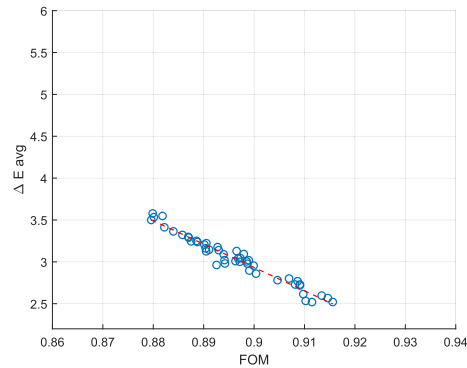

 (d) *In situ* data, correlation=-0.978

 Figure 5. Signal dependent noise FOM versus  $\Delta E$  at a noise slope of  $\gamma = 0.8$ .

Figure 5 shows the results when using the FOM that accounts for signal dependent noise, which involves the use of Eq. (16). The results are quite good for all four spectral data sets in that the slope of the relationship between the FOM and  $\Delta E$  are similar, and all have high levels of correlation. Fig. 4(a)–4(c) are similar to Fig. 5(a)–5(c) in terms of their correlation numbers. A clear difference exists though for the *in situ* data set. The *in situ* data looks good when we account for the signal dependent noise (Fig. 5d) compared to the case that assumes a signal independent noise model (Fig. 4d).

The difference between Fig. 4(d) and Fig. 5(d) prompted an investigation into the source of the difference. It was found that the *in situ* data set includes samples that contain relatively dark luminance values, which are not present in the other data sets. Figure 6 displays CIELAB gamut cross sections of the four data sets. From this figure, we can see that the *in situ* set of Fig. 6(d) contains a number of spectra with  $L^*$  values below 15 (approximately 5% of the spectra). These are dark compared to the black values in the color targets and textiles. Examination of these spectra showed they could have relatively high values in the UV and IR ends of the spectrum, but little in the visible range covered by the CIE color matching functions.

Investigation of the difference between  $\tilde{S}_{sd}$  and  $\tilde{S}_n$  for the *in situ* data set showed that Sharma's FOM estimates a significantly lower SNR for the dark samples compared to the

measure that accounts for the signal dependent noise. The signal independent average noise produces a very low SNR for the dark samples that affects the estimation process and degrades the overall FOM. As such, it ends up relating poorly to the  $\Delta E$  values that occur with the signal dependent noise model. To demonstrate the issue, we removed dark samples (those with  $L^* < 15$ ) from the *in situ* data set and computed the original FOM (with the nonlinear adjustment) with the version that uses  $\tilde{S}_{sd}$ . The results are shown in Figure 7 which show similar levels of correlation. We also verified the dark sample effect by adding 5% dark spectra to the textiles database, which resulted in the standard FOM measure to perform poorly.

#### 4. CONCLUSION

This work investigated how well goodness measures for the spectral sensitivity of color measuring devices relate to color performance. The approach considered a realistic camera model that included signal dependent noise, which is dominant in virtually all cameras. It was shown that the Vora value does a poor job in relating to  $\Delta E$ . It was also shown that Sharma's FOM has issues if the spectral data set includes samples that have low luminance levels. Use of an FOM that accounts for signal dependent noise was shown to help improve the correlation with  $\Delta E$  performance, in particular if the device is to be used for a wide range

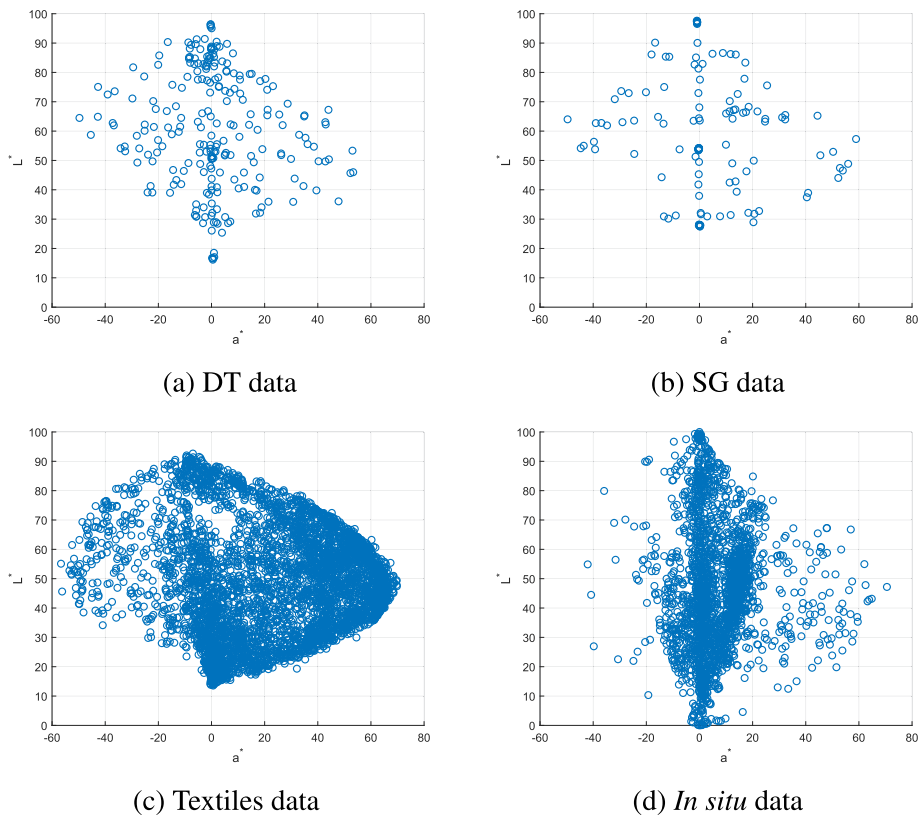


Figure 6.  $L^* a^*$  gamut cross sections of spectra.

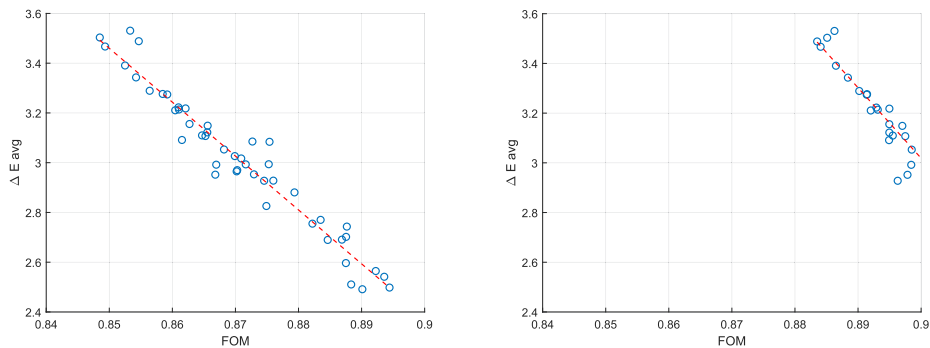


Figure 7. *In situ* results with dark spectra removed.

of luminance values. This signal dependent noise FOM should prove useful in the determination of optimal spectral responses for color measuring devices and in comparing the colorimetric performance of different devices.

#### ACKNOWLEDGMENT

The authors would like to thank Dietmar Wüller for providing access to his database of spectral radiant measurements [26]. In addition, they would like to thank Professor Shoji Tominaga for access to the mobile phone camera spectral sensitivities [24].

#### REFERENCES

- 1 P. L. Vora and H. J. Trussell, "Mathematical methods for the analysis of color scanning filters," *IEEE Trans. Image Process.* **6**, 321–327 (1997).
- 2 P. L. Vora and H. J. Trussell, "Mathematical methods for the design of color scanning filters," *IEEE Trans. Image Process.* **6**, 312–320 (1997).
- 3 S. Quan, N. Ohta, and N. Katoh, "Optimization of camera spectral sensitivities," *Proc. IS&T/SID CIC8: Eighth Color Imaging Conf.* (IS&T, Springfield, VA, 2000), pp. 273–278.
- 4 H. J. Trussell, A. O. Ercan, and N. G. Kingsbury, "Color filters: When "optimal" is not optimal," *2016 IEEE Int'l. Conf. Image Process, Phoenix, AZ* (IEEE, Piscataway, NJ, 2016), pp. 3987–3991.

- <sup>5</sup> G. Sharma and H. J. Trussell, "Figures of merit for color scanners," *IEEE Trans. Image Process.* **6**, 990–1001 (1997).
- <sup>6</sup> G. D. Finlayson, Y. Zhu, and H. Gong, "Using a simple colour pre-filter to make cameras more colorimetric," *Proc. IS&T CIC26: Twenty-Sixth Color and Imaging Conf.* (IS&T, Springfield, VA, 2018), pp. 182–186.
- <sup>7</sup> M. J. Vrhel, "Improved camera color accuracy in the presence of noise with a color prefilter," *Proc. IS&T CIC28: Twenty-Eighth Color and Imaging Conf.* (IS&T, Springfield, VA, 2020), pp. 187–192.
- <sup>8</sup> M. J. Vrhel and H. J. Trussell, "Selection of optimal external filter for colorimetric camera," *Proc. IS&T CIC29: Twenty-Ninth Color and Imaging Conf.* (IS&T, Springfield, VA, 2021), pp. 141–147.
- <sup>9</sup> G. D. Finlayson and Y. Zhu, "Designing color filters that make cameras more colorimetric," *IEEE Trans. Image Process.* **30**, 853–867 (2021).
- <sup>10</sup> H. J. Trussell and M. S. Kulkarni, "Sampling and processing of color signals," *IEEE Trans. Image Process.* **5**, 677–681 (1996).
- <sup>11</sup> M. J. Vrhel and H. J. Trussell, "Filter considerations in color correction," *IEEE Trans. Image Process.* **3**, 147–161 (1994).
- <sup>12</sup> M. J. Vrhel, H. J. Trussell, and J. Bosch, "Design and realization of optimal color filters for multi-illuminant color correction," *J. Electron. Imaging* **4**, 6–14 (1995).
- <sup>13</sup> M. J. Vrhel and H. J. Trussell, "Optimal color filters in the presence of noise," *IEEE Trans. Image Process.* **4**, 814–823 (1995).
- <sup>14</sup> M. Wolski, C. Bouman, J. P. Allebach, and E. Walowit, "Optimization of sensor response functions for colorimetry of reflective and emissive objects," *IEEE Trans. Image Process.* **5**, 507–517 (1996).
- <sup>15</sup> G. Sharma, H. J. Trussell, and M. J. Vrhel, "Optimal nonnegative color scanning filters," *IEEE Trans. Image Process.* **7**, 129–133 (1998).
- <sup>16</sup> H. Kuniba and R. S. Berns, "Spectral sensitivity optimization of color image sensors considering photon shot noise," *J. Electron. Imaging* **18**, 1–14 (2009).
- <sup>17</sup> M. Parmar and S. J. Reeves, "Selection of optimal spectral sensitivity functions for color filter arrays," *IEEE Trans. Image Process.* **19**, 3190–3203 (2010).
- <sup>18</sup> D. Ng, J. P. Allebach, M. Analoui, and Z. Pizlo, "Non-contact imaging colorimeter for human tooth color assessment using a digital camera," *J. Imaging Sci. Technol.* **47**, 531–542 (2003).
- <sup>19</sup> J. Farrell, D. Sherman, and B. Wandell, "How to turn your scanner into a colorimeter," *Proc. IS&T's Tenth Int'l. Congress on Advances in Non-Impact Printing Technologies* (IS&T, Springfield, VA, 1994), pp. 579–581.
- <sup>20</sup> H. E. J. Neugebauer, "Quality factor for filters whose spectral transmittances are different from color mixture curves, and its application to color photography," *J. Opt. Soc. Am.* **46**, 821–824 (1956).
- <sup>21</sup> P. L. Vora and H. J. Trussell, "Measure of goodness of a set of color scanning filters," *J. Opt. Soc. Am. A* **10**, 1499–1508 (1993).
- <sup>22</sup> H. J. Trussell and R. Zhang, "The dominance of Poisson noise in color digital cameras," *2012 IEEE Int'l. Conf. Image Process* (IEEE, Piscataway, NJ, 2012), pp. 329–332.
- <sup>23</sup> J. Jiang, D. Liu, J. Gu, and S. Süssstrunk, "What is the space of spectral sensitivity functions for digital color cameras?," *2013 IEEE Workshop on Applications of Computer Vision (WACV)* (IEEE, Piscataway, NJ, 2013), pp. 168–179, Camera data accessed October 2021.
- <sup>24</sup> S. Tominaga, S. Nishi, and R. Ohtera, "Measurement and estimation of spectral sensitivity functions for mobile phone cameras," *Sensors* **21**, 4985 (2021).
- <sup>25</sup> A. Shams-Nateri, "Measuring reflectance spectra of textile fabrics by scanner," *J. Text. Sci. Eng.* **102**, 1–13 (2011).
- <sup>26</sup> D. Wüller, "In situ measured spectral radiation of natural objects," *Proc. IS&T/SID CIC17: Seventeenth Color and Imaging Conf.* (IS&T, Springfield, VA, 2009), pp. 159–163.
- <sup>27</sup> H. J. Trussell and R. Shamey, "Accurate colorimetric images using LEDs," *J. Electron. Imaging* **29**, 1–16 (2020).